Histological and immunohistochemical study on the effect of Carbon tetrachloride on kidney of adult male albino rats

Rania M. Al Adly[a], Amal T. Abou-Elghait[b,c], Fatma Y. Meligy[b,f] , Eman Radwan[d,e] Eman A. Abdelrahim[a]

[a]Histology and Cell Biology Department, Faculty of Medicine, South Valley University, Qena, 83523, Egypt.
[b]Histology and Cell Biology Department, Faculty of Medicine, Assuit University, Assuit,71515.Egypt.
[c]Histology and Cell Biology Department, Faculty of Medicine, Sphinx University, New Assuit City, 10, Assuit, Egypt.
[d]Department of Biochemistry , Sphinx University, New Assuit City, 10, Assiut, Egypt.
[e]Department of Medical Biochemistry , Faculty of Medicine, Assuit University, Assiut,71515, Egypt.
[f]Department of Restorative Dentistry and Basic Medical Sciencies, Faculty of Dentistry,University of Petra, Amman, 11196, Jordan.

Abstract

Background: Chronic kidney disease (CKD) is a major worldwide public health concern. A hallmark that is shared by all progressive chronic kidney diseases is tubulointerstitial fibrosis. Prolonged exposure to high amounts of carbon tetrachloride (CCL4), especially in vapor form, can cause kidney injury. Autophagy played a major role in stress adaptation and organ homeostasis maintenance. Impaired autophagy has frequently been associated with renal damage and fibrosis**.**

Objectives: The aim of this work is to assess the kidneys' histopathological response to CCl4 and the potential involvement of autophagy in this disease.

Materials and Methods: Twenty adult male albino rats were randomly divided into two equal groups (10 rats, each); Group 1: Control group. Group 2: The CCl4 group, rats were received CCl4, 1.5 mg/kg twice weekly subcutaneously (S.C) for 12 weeks. After sacrifice, kidneys were taken from all animal groups and processed for light microscopy, Immunological studies, Biochemical tests and statistical analysis were done.

Results: When CCL4 was administered, the kidney tissue underwent histological alterations, including areas of tissue breakdown, inflammatory cell infiltration, congestion and fibrosis.

Conclusion: Renal adverse effects, including inflammation, degeneration, and subsequently fibrosis, were brought on by CCl4 treatment for a duration of 12 weeks. One of the key processes via which CCl4 damages tissue is autophagy suppression.

Keywords: CCL4; Renal fibrosis; Autophagy.

***Correspondence**: rania_mohamed7347@med.svu.edu.eg

DOI: 10.21608/SVUIJM.2024.283218.1838
Received: 1 May, 2024.
Revised: 7 May, 2024.
Accepted: 24 May, 2024.
Published: 24 May, 2024
Cite this article as: Rania M. Al Adly, Amal T. Abou-Elghait, Fatma Y. Meligy , Eman Radwan Eman A. Abdelrahim.(2024). Histological and immunohistochemical study on the effect of Carbon tetrachloride on kidney of adult male albino rats. *SVU-International Journal of Medical Sciences*. Vol.7, Issue 1, pp: 939-953.

Introduction

Renal fibrosis is the main histologic characteristic of CKD. Worldwide, about 10% of persons suffer from CKD **(Bikbov et al., 2020).** The disease is becoming more common each year and is one of the main illnesses threatening the public's health. The US Centers for Disease Control and Prevention estimated that 7% of elderly people may eventually develop end-stage renal disease (ESRD), which necessitates kidney transplantation or dialysis to survive **(Keith et al., 2004).** Target organs primarily impacted by xenobiotics are the liver and kidney **(Aziz et al., 2022).** CCl4 is a frequently employed toxin that is utilized to induce organ toxicity in experimental settings. Covalent binding to protein membranes and increased lipid peroxidation, which results in tissue damage, are two distinct mechanisms by which the chemical molecule CCl4 facilitates oxidative stress and cell death **(Morsy et al., 2021).** A common solvent in the chemical industry is CCl4. It is also widely documented to have harmful effects on the kidneys, liver, brain and lungs. Serious health risks are imposed by it **(Baig and Khan, 2023).**

Almost all eukaryotic cells have basal levels of autophagy, which is responsible for maintaining cellular homeostasis **(Li et al., 2021).** Autophagy is a highly conserved lysosomal protein degradation system that breaks down protein aggregates, damaged organelles, and even invasive infections **(Mizushima et al., 2008).** Moreover, autophagy is a required adaptive process for cell survival and can be triggered by metabolic, genotoxic, or hypoxic stress signals **(Mizushima and Levine, 2020).**

Autophagy provides protection against injury to renal cells **(Tan et al., 2018).** On the other hand, a lack of autophagy increases the kidney's susceptibility to injury, increasing the risk of renal fibrosis, decreased renal function, and an accumulation of damaged mitochondria **(Gui et al., 2021).** However, other studies have shown that persistently inducing autophagy is harmful to the kidney after significant injury, leading to renal cell senescence and promoting renal fibrosis through the release of profibrotic cytokines **(Zheng et al., 2019).**

The aim of the current work is to assess the kidneys' histopathological response to CCL4 and the potential involvement of autophagy in this disease.

Materials and Methods

I- Chemicals

CCl4 solution was purchased from Sigma Co., St. Louis, USA.

Olive oil was purchased from a local supermarket.

Antibody against P62 was obtained from Cell Signaling (Danvers, MA, USA).

II- Animals

A total of 20 adult male albino rats, 8 weeks of age, 200-250 gm in weight, were bought from the Assiut University animal house and kept in hygienic, roomy cages, with up to 4 rats per cage. The rats were kept in an aerated room with a natural light-dark cycle of 12 hours, with water and regular rat pellets as their meal. The temperature was kept at 25 ± 5˚C. Qena Faculty of Medicine, South Valley University, Egypt's Institutional Animal Research Committee accepted the experimental protocol, and it was conducted in accordance with the ethical guidelines that were suggested by the same university. The full ethical committee approval code is: (SVU, MED, HIS002, 2, 6/2021, 208).

Experimental Groups: The rats were randomly divided into two groups, ten animals each as follows: **Group 1 (control group):** Rats received distilled water orally at a dose of 0.5mg/kg daily by intragastric tube.

Group 2: (CCL4 group): Rats received CCL4 S.C dissolved in olive oil in 50:50 percentage at a dose of 1.5 ml/kg twice weekly for 12 weeks **(Barakat and Almundarij, 2020).** At the end of the experiment, all animals were sacrificed under general anaesthesia, and kidneys

from each animal group were removed by decapitation via a median abdominal incision. The kidneys were then processed for immunological research, biochemical testing, statistical analysis, and light microscopy.

For Light microscopy: Kidney specimens were extracted from each group, preserved in 10% formalin, cleaned in 70% alcohol, dried using increasing alcohol concentrations, embedded in paraffin, sectioned using a microtome at a thickness of 5 μm, and stained with the subsequent dyes:

1- Routine hematoxylin and eosin (H&E) stain: for routine histological examination.
2- Masson's trichrome stain: for demonstration of collagen fibers. All staining methods were done according to Bancroft and Layton **(Bancroft and Layton, 2013).**
3- P62 positive cell recognition via IHC staining. Using a Leica microscope equipped with a digital camera, pictures of the examined slides were taken.

Biochemical study: First, blood samples were centrifuged for 15 minutes at 3000 rpm per minute (rpm). The non-hemolyzed, transparent supernatant sera were extracted and stored at -20˚C until needed for examination. Spectral diagnostic kits (Spectrum®, Hannover, Germany) were used to measure the amounts of blood urea, serum creatinine, blood albumin, and serum uric acid (mg/dL). Commercial kits were used to test serum albumin (gm/dl).

Morphometric study: Masson's Trichrome stained sections were morphometrically analysed. The mean percentage area of collagen fibers was measured in Masson's trichrome stained sections in all groups by using image j software. The number of P62 positive cells were compared in the groups of the study. A computerized image analyzer system software (Leica Q 500 MCO, Leica) and a camera attached to a Leica universal microscope at the Histology Department, Faculty of Medicine, Assiut University were used.

Statistical analysis

Data was collected, coded, revised, and entered into the Statistical Package for Social Science (IBM SPSS) version 27. Data were tested for normality using the Kolmogorov-Smirnov and Shapiro-Wilk tests. The data were presented as mean ± standard deviations (SD) for the numerical variables with parametric distribution.

Student t-test was used in the comparison between two groups with quantitative data and parametric distribution.

The p-value was deemed significant as follows:• $p > 0.05$: Nonsignificant (NS) • $p < 0.05$: Significant (S)• $p < 0.01$: Highly significant (HS).

Results

H&E-stained sections

H&E-stained kidney slices from control rats demonstrated normal renal cortex architecture (**Fig. 1**), with renal corpuscles featuring glomeruli with normal cellularity encircled by Bowman's capsule and capsular spaces. Numerous proximal convoluted tubules (PCT) lined by pyramidal cells and distal convoluted tubules (DCT) lined by cubical cells encircle renal corpuscles. These cells' nuclei are basophilic, while their cytoplasm is acidophilic (**Fig. 2**).

When compared to the control rats, the kidney experienced significant histological damage as a result of CCL4 treatment. Investigating renal cortical slices from rats treated with CCl4 revealed damaged Malpighian corpuscles, exhibiting glomeruli that are deformed and shrunken, with some capsular spaces becoming wider and certain Bowman's capsules becoming thicker (**Figs. 3,4 and 5**).

The tubular epithelial cells displayed hazy (vacuolar) swellings, degeneration, and shedding, while the tubules appeared dilated with uneven walls and casts in their lumens. In addition to interstitial hemorrhages, the PCT brush borders have disappeared (**Fig. 6**). Additionally,

inflammatory cell infiltrations were found (**Fig. 7**).

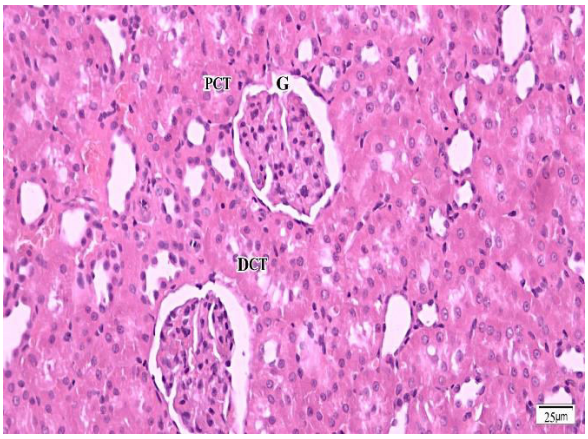

Fig. 1. Photomicrograph of kidney section stained with hematoxylin-eosin stain from control rats, showing normal histological architecture of the rat kidney cortex, normal glomeruli (G), normal Bowman's space, normal PCT and DCT (H&E, x400) **.**

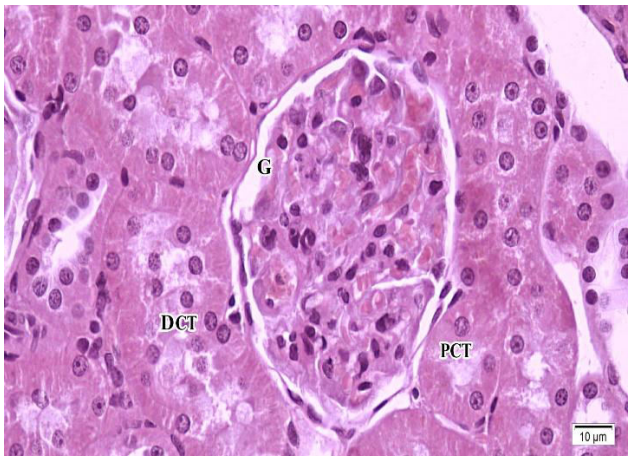

Fig. 2. Photomicrograph of kidney section of control group at higher magnification showing normal histological architecture of the rat kidney cortex, normal glomeruli (G), normal Bowman's space, normal PCT and DCT (H&E, x1000).

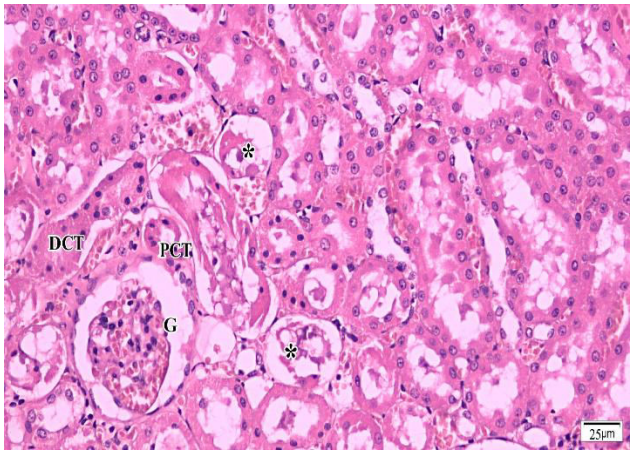

Fig. 3. Photomicrograph of CCL4 treated kidney section showing loss of normal architecture of renal cortex. Malpighian corpuscles display shrunken and distorted glomeruli (G) with widening of the capsular spaces, the renal tubules are destroyed (*) (H&E, x400).

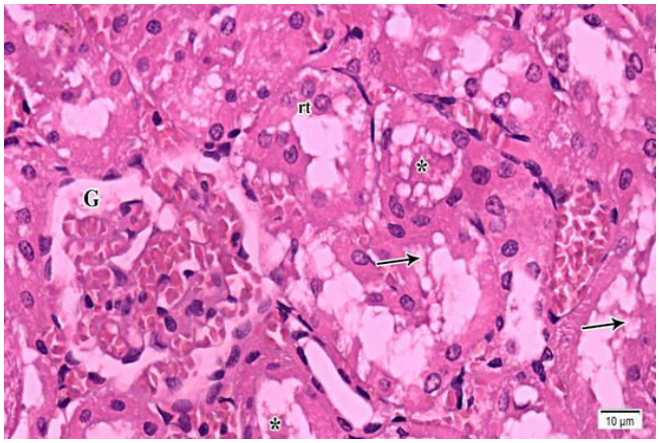

Fig. 4. Photomicrograph of CCL4 treated kidney section at higher magnification showing distorted and congested glomerulus (G). The surrounding proximal and distal tubules (rt) are dilated, irregular with vacuolar degeneration of their lining cells (arrows), some lumens contain casts (*) may be shredded and necrotic epithelium (H&E, x1000).

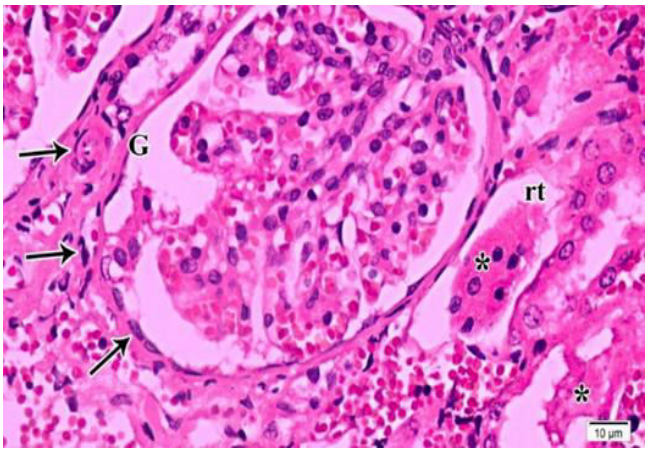

Fig. 5. Photomicrograph of CCL4 treated kidney section showing renal tubules (rt) with vacuolar degeneration of their lining cells, some lumens contain casts (*), may be shredded and necrotic epithelium. There is thickening of Bowman's capsule (arrows) (H&E, x1000).

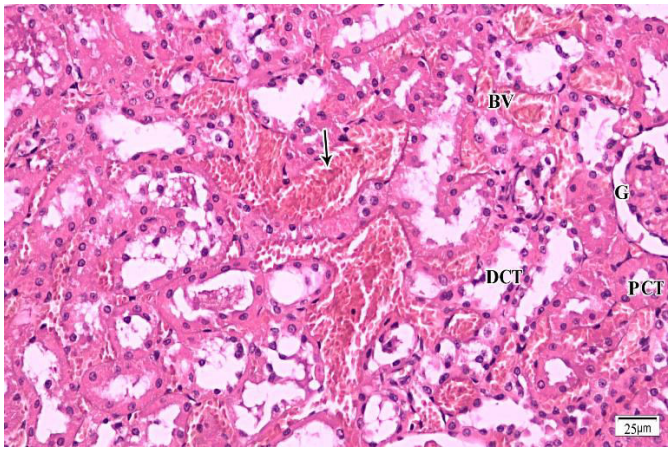

Fig. 6. Another photomicrograph of CCL4 treated kidney section showing destructed renal tubules, congestion of blood vessels (BV) and interstitial hemorrhages (arrow) (H&E, x400).

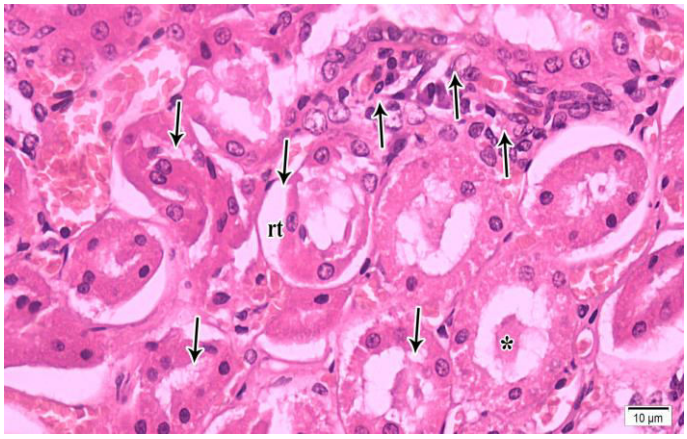

Fig. 7. Photomicrograph of CCL4 treated kidney section showing dilated renal tubules (rt) with vacuolar degeneration of their lining cells (downward arrows), some lumens contain casts (*), may be shredded and necrotic epithelium, the upward arrows refers to inflammatory cell infiltrations (H&E, x1000) .

Masson's trichrome-stained sections

The interstitial connective tissue composition of the renal tissues varied noticeably between the treated and control sections. Little interstitial connective tissue was visible surrounding the glomeruli and tubules in the control sections of the renal tissues stained with Masson's trichrome (**Fig. 8**).

The interstitial connective tissue content greatly increased in the renal tissues of rats treated with CCl4; this increase was mainly seen in the intra-glomerulus, around the renal corpuscles, in the intertubular spaces, and around the blood vessels (**Fig. 9**).

.

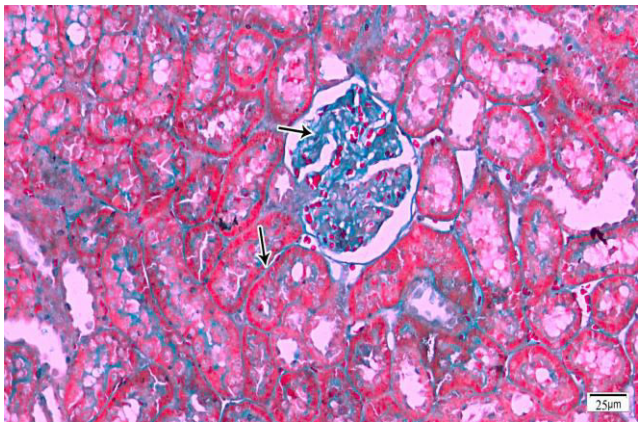

Fig. 8. Photomicrograph of kidney sections stained with Masson's trichrome stain from control group showing scanty interstitial connective tissue and low collagen content surrounding the glomeruli and tubules (arrows) (Masson's trichrome, x400).

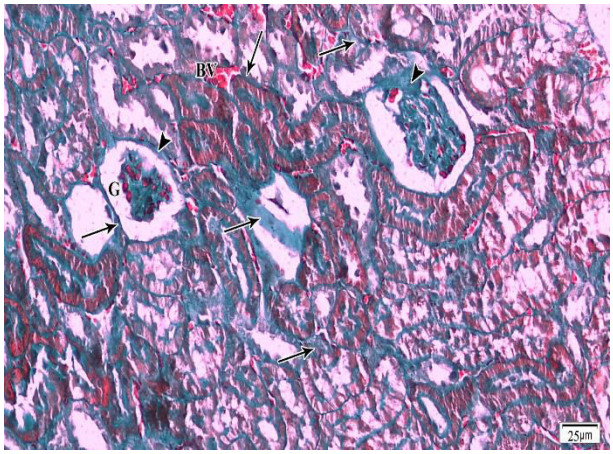

Fig. 9. Photomicrograph of CCl4 treated sections exhibited an extensive increase in the connective tissue content in the glomeruli (G), peri-glomerular spaces (arrowheads), surrounding the blood vessels (BV), and in the intertubular spaces (arrows) (Masson's trichrome, x400).

The mean percentage area of collagen fibers was calculated using Image J software. Between the test groups, there was a statistically significant difference ($p<0.001$). The percentage of fibrosis was found to be considerably higher in group 2 (CCL4) compared to group 1 (control) (26.6460 ± 2.91320 % vs. 8.5510 ± 1.03218%, respectively; $p< 0.001$) (**Table.1, Chart.1**).

Table 1. Autophagy marker (P62) and fibrosis among the studied groups

Parameters	Group (1)	Group (2)	P value
	Mean ± SD	Mean ± SD	
Anti-P62 (%)	13.8123 ± 2.06323	33.2946 ± 3.42240	< 0.001*
Fibrosis area (%)	8.5510 ± 1.03218	26.6460 ± 2.91320	< 0.001*

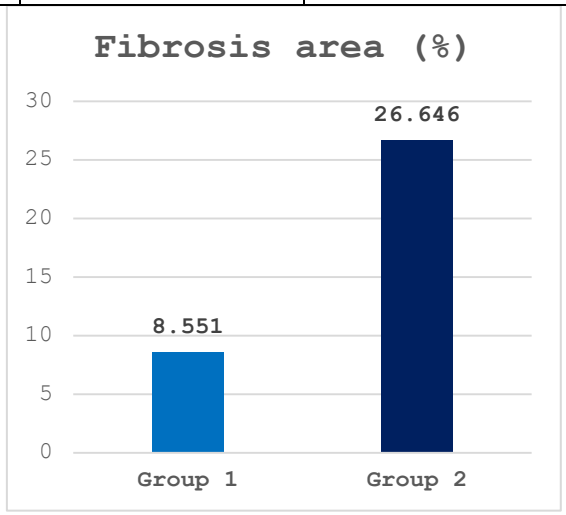

Chart 1. Mean percentage of the fibrosis area among the tested groups.

Immunohistochemical observations for P62 (Autophagy marker):

As compared to control rats (**Fig. 10**), the CCl4-treated group displayed more cytoplasmic immunoreactivity, as evidenced by the brown color in the renal

tissues of the rats (**Fig. 11**).This was according to the results of image analysis for P62 expression.

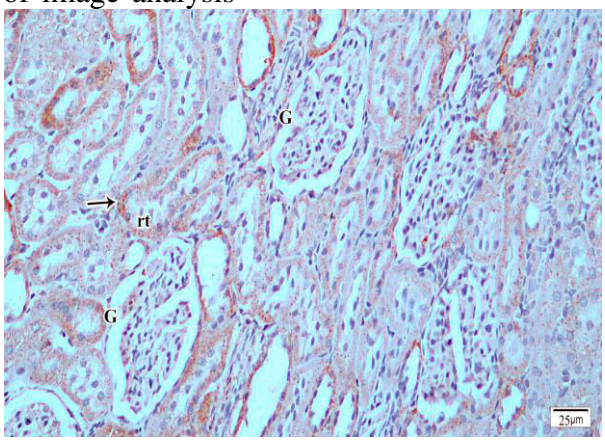

Fig. 10. Photomicrograph of kidney tissue sections stained with Anti P62 immunostaining from a control rats showed low levels of immunoreactivity for P62 in the renal tubules (rt) as shown by the brown staining (x400).

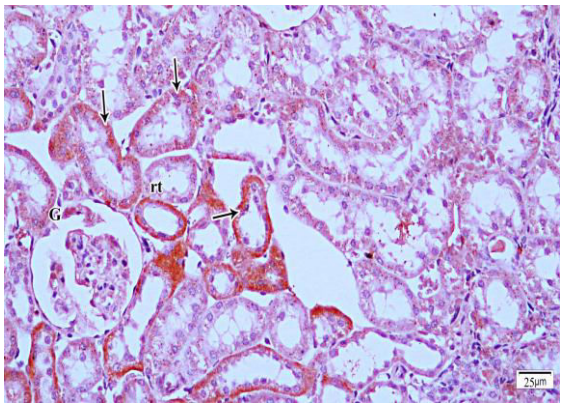

Fig.11. Photomicrograph of kidney tissues of the CCL4-treated group exhibited stronger and widespread immunoreactivity for P62 compared to previous group as shown by the brown coloration in the renal tissues (x400).

There was a statistically significant difference between the control and CCL4 groups regarding autophagy marker; p< 0.001. Anti-P62 was significantly lower in Group 1(control) than in Group 2 (CCl4) (13.8123 ± 2.06323 vs. 33.2946 ± 3.42240, respectively, p< 0.001), (**Table.1, Chart .2**).

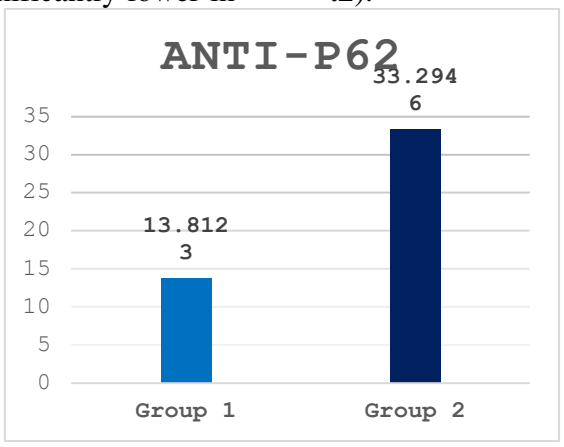

Chart 2. Mean of the anti-P62 among the tested groups.

Kidney function tests

The nephrotoxicity induced by CCl4 was demonstrated by measuring renal chemistry. There was a statistically significant difference between the tested groups (p<0.001). The higher blood urea, creatinine and uric acid levels were found in CCL4 group which was significantly higher than control group (p<0.001). The lower albumin level reported in CCL4 group was significantly lower than control group (p<0.001).(Table 2). Serum urea level was significantly higher among group 2 than group 1 (49.8760 ± 4.14679 mg/dL vs. 20.1760 ± 0.92790 mg/dL, respectively, p< 0.001) (**Table 2, Chart.3**).

Table 2. Renal chemistry among the tested groups* Student t-test

Parameters	Group (1)	Group (2)	P value
	Mean ± SD	Mean ± SD	
Urea (mg/dL)	20.1760±0.92790	49.8760± 4.14679	<0.001*
Creatinine (mg/dL)	0.8280 ± 0.08230	2.4660 ± 0.44290	<0.001*
Uric acid (mg/dL)	1.7160 ± 0.11481	2.7320 ± 0.17106	< 0.001*
Albumin (g/dL)	3.5740 ± 0.06310	2.3660 ± 0.31038	< 0.001*

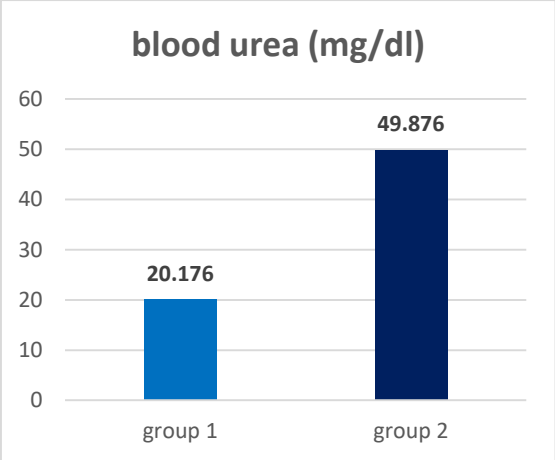

Chart 3. Column graphic presentation of the mean of blood urea level among the tested groups.

Serum creatinine was significantly higher among group 2 than group 1 (2.4660 ± 0.44290 mg/dL vs. 0.8280 ± 0.08230 mg/dL, respectively, p< 0.001) ,(**Table 2, Chart 4**). Serum uric acid was significantly higher among group 2 than in group 1 (2.7320 ± 0.17106 mg/dL vs. 1.7160 ± 0.11481 mg/dL, respectively, p<0.001), (**Table 2, Chart 5**). Finally, Albumin level was lower in group 2 than in group 1 (2.3660 ± 0.31038 g/dL vs. 3.5740 ± 0.06310 g/dL, respectively, p< 0.001), (**Table.2, Chart.6**).

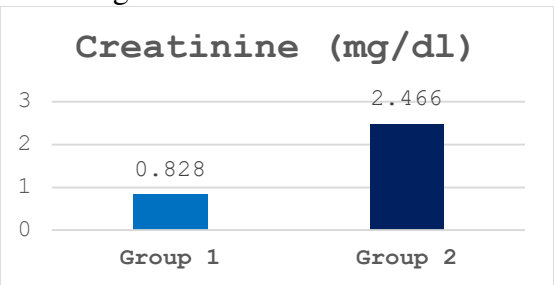

Chart 4. Column graphic presentation of the mean of the serum creatinine level among the tested groups.

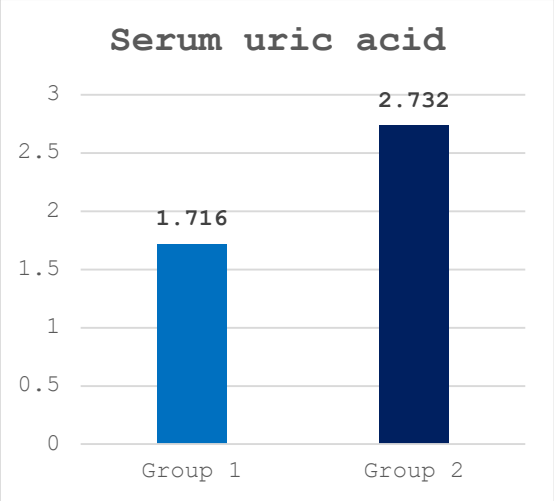

Chart 5. Column graphic presentation of the mean of the serum uric acid level among the tested groups.

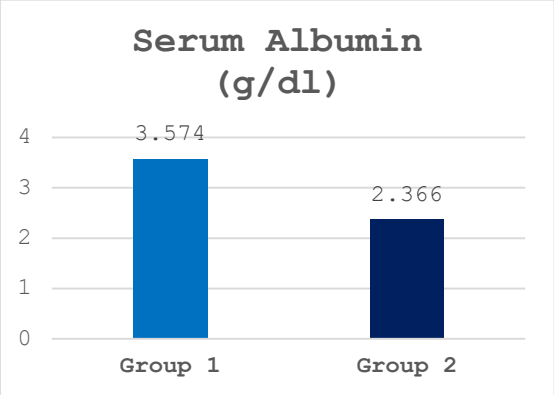

Chart 6. Column graphic presentation of the mean of the serum albumin level among the tested groups.

Discussion

In this work, the damaging consequences of a 12-week CCL4 therapy were examined in adult male albino rat kidneys, as well as the possible impact of autophagy on these outcomes.

Based on our research, H&E-stained kidney tissue slices revealed smaller, deformed renal corpuscles with expanded capsular spaces, thickened bowman's capsules in certain instances, and hemorrhages in the majority of the glomeruli. The majority of renal tubules were deformed, showing cloudy swellings and degeneration of epithelial cells. In their lumens, there were casts or necrotic epithelium. A thicker basal lamina was present in some tubules. Renal blood vessels were also congested with areas of interstitial hemorrhages.

The main target organs impacted by xenobiotics are the liver and kidneys **(Aziz et al., 2022).** CCl_4 is a chemical compound that promotes the process of oxidative stress and cell destruction. It is still possible to find CCl4 in firefighting equipments (extinguishers), pesticides, and cereals that have been disinfected (fumigated). CCl4 is an established experimental drug for the creation of hepatotoxicity and neprotoxicity models, since it is known to cause liver and kidney fibrosis in humans **(Yeh et al., 2013).**

The process by which CCl4 converts to highly toxic free radicals of trichloromethyl radicals (•CCl) and trichloromethyl peroxyl radical (•CCl_3O2)

via the cytochrome P450 enzyme can be used to explain the oxidative damage produced by lipid peroxidation that occurs in tissues as a result of CCl4 **(Que et al., 2022).**

Lipid peroxidation occurs as a result of these dangerous free radicals in phospholipid-rich membrane-like structures such as the mitochondria and endoplasmic reticulum (ER). Lipid peroxidation caused by CCl4 results in ER stress, mitochondrial stress, and oxidative stress. Free radicals initiate several biological processes, such as necrosis, autophagy, ferroptosis, and apoptosis **(Unsal et al., 2021).**

Our results regarding CCL4 destructive effects align with a number of earlier studies. **Ma et al. (2021)** demonstrated that CCL4 caused an inflammatory response and renal fibrosis in mice by lowering the amount of Nuclear factor erythroid 2-related factor 2L (Nrf2), a critical regulator of antioxidant proteins involved in the control of antioxidant gene transcription and the regulation of oxidative stress, fibrosis, inflammation, and apoptosis. **Alzahrani et al. (2024)** reported lowered levels of catalase (CAT) and superoxide dismutase (SOD), indicators of liver and kidney tissues antioxidant capacity, in rats subjected to CCL4, but the level of malondialdehyde (MDA), a pro-oxidative marker, was markedly increased. **El-Refai et al. (2024)** documented reduced levels of glutathione (GSH), a potent endogenous antioxidant, and the total antioxidant capacity (TAC) in relation to hepatorenal damage caused by CCl4. Interleukin-6 (IL-6), tumor necrosis factor-α (TNF-α), TNF-1β, and interleukin-10 (IL-10) were among the inflammatory cytokines that **Shi et al. (2024)** demonstrated their greater amounts, causing fibrosis to develop in CCl4 rats. Meanwhile, **Zhao et al. (2024)** found that CCl4 increased liver fibrosis markers; hyaluronic acid (HA), collagen type IV (CIV), N-terminal propeptide of type III procollagen (PIIINP), and laminin (LN), oxidative stress (SOD, MDA, GSH), and inflammatory factors (IL-6, TNF-α).

The last stage of CKD is kidney fibrosis, during which renal tissue regeneration takes place in interstitial tubules by forming a significant amount of extracellular matrix (ECM) **(Ruiz-Ortega et al., 2020).** Renal tubular epithelium-derived myofibroblasts create ECM. Epithelial mesenchymal transition; EMT, is the term for this process that moves the tubular epithelium in an interstitial course **(Sheng and Zhuang, 2020).** CCl4 prolongs damage to kidney tubules and glomerular cells, which results in a constant generation of pro-inflammatory cytokines like TNF-α and IL-6 **(Lin and Hsu, 2020).** Overexposure to TNF-α and IL-6 impairs normal regeneration and triggers the EMT process **(Li et al., 2016).**

Our study's CCL4 and control groups have notably varied interstitial connective tissue compositions. The Masson's trichrome stain was applied to demonstrate this, and Image J software was utilized to provide the morphometric confirmation of the findings by calculating the mean percentage area of collagen in each experimental group. Rats subjected to CCL4 showed an expansion of their ECM.

According to **Ma et al. (2021), Lamia et al. (2021),** and **Singh et al. (2024),** CCL4 plays a significant role in the beginning of fibrosis in rats which supported our findings. It was found by **Susilo et al . (2022)** that α-SMA expression (the key indicator of myofibroblast activation) was increased by CCl4.

Regarding the impact of CCL4 on renal chemistry, our results aligned with those of **Baig and Khan (2023)** and **Ben Mansour et al. (2024),** who documented renal damage caused by CCL4 in rats. In contrast to the control group, it was clear that CCl4 decreased blood albumin and increased blood levels of urea, uric acid, and creatinine. They states that glomerular cell and kidney tubule toxicity are caused

by the effects of CCl4 metabolism in the body.

Numerous renal illnesses, including renal fibrosis, have been linked to the pathophysiology of autophagy, an important stress-responsive system **(Liang et al., 2022).** Autophagy plays a significant role in adult renal resident cells and is intimately associated with the advancement of renal fibrosis **(Dai et al., 2022).** Autophagy can be triggered by a variety of cellular stresses, such as invasive infections, hypoxia, reactive oxygen species (ROS), stress on the ER, DNA damage, and immunological signals. However, it is unknown exactly how autophagy functions in various renal cell types during renal fibrosis **(Shu et al., 2021).**

The ubiquitin-proteasome system (UPS) and autophagy, are two important quality control processes that facilitate the effective removal of damaged proteins and protein aggregates. Both pathways are essential for maintaining cellular homeostasis **(Pohl and Dikic, 2019).** Autophagy facilitates the removal of cellular ubiquitinated aggregates, while the UPS primarily uses proteasomes to break down ubiquitinated misfolded proteins (**Mizushima, 2018).** Selective autophagic clearance of ubiquitinated proteins is a UPS compensatory strategy when proteasome activity decreases with age or in response to environmental stressors **(Matsumoto et al., 2011).** The purpose of the current study was to better understand how kidney autophagy is affected by CCL4 administration, so we measured the level of P62 (autophagy marker) in the tested groups.

Autophagy receptors mediate selective autophagy by identifying and reserving certain cargo for the autophagosome. The autophagosome then merges with a lysosome, where ubiquitinated proteins are hydrolyzed by lysosomal hydrolases **(Lamark and Johansen, 2021).**

P62 is an autophagy receptor that takes role in the autophagic removal of ubiquitinated proteins before autophagy activation degrades it and its cargo **(Kumar et al., 2022).**

A Phox1 and Bem1p (PB1) domain, a microtubule-associated protein 1 light chain 3 (LC3)-interacting region (LIR), and a ubiquitin associated (UBA) domain are among the several domains that make up P62. During selective autophagy, P62 interacts with LC3 on autophagosomes through its LIR domain and uses its UBA domain to bind to ubiquitinated proteins. This interaction eventually causes ubiquitinated proteins to be degraded by lysosome fusion **(Isogai et al., 2011).** Through the formation of insoluble cytoplasmic inclusions called P62 bodies, P62 in cells facilitates the assembly and removal of ubiquitinated proteins **(Sun et al., 2018).** It has been demonstrated that a number of P62-binding partners and posttranslational P62 changes, change the behavior of P62 droplets which controls P62-mediated selective autophagy **(Kageyama et al., 2021, Feng et al., 2022).**

It is not known how autophagosomes effectively trap phase-separated P62 droplets, despite the fact that P62-mediated selective clearance of ubiquitinated proteins depends on the interaction of membrane-associated LC3 with the LIR of P62 so P62 decreases when autophagy is activated **(Feng et al., 2022).**

Our study showed that, in comparison to the control group, rats exposed to CCL4 had significantly higher levels of P62 protein in their kidney tissues. This shows that renal fibrosis due to CCL4 administration has the effect of inhibiting autophagy. **Chen et al. (2024)** examined autophagy and ferroptosis-related gene targets in the renal tissues of patients with CKD and discovered a substantial upregulation of P62 mRNA expression in this condition. Their results were consistent with our findings.

Numerous approaches have been taken to investigate the function of autophagy in fibrosis **(Tang et al., 2020).** Autophagy

shields tubular cells from apoptosis and stimulates cellular regeneration following acute kidney damage **(Lin et al., 2019).** Nevertheless additional research has discovered that persistently triggering autophagy is detrimental to the kidney following severe damage, resulting in the senescence of renal cells and encouraging renal fibrosis by releasing profibrotic cytokines **(Zheng et al., 2019).** Therefore, the specific role of autophagy in renal fibrosis remains unknown.

Conclusion

Treatment with CCl4 for a period of 12 weeks, resulted in unfavorable consequences on the kidneys, such as inflammation, degeneration and eventually fibrosis. The downregulation of autophagy in renal tissues exposed to CCL*4* is one of the main mechanisms by which the chemical causes tissue damage. This was observed in our research by an increase in P62 level.

References

- **Alzahrani SA , Bekhet GM , Ammar RB , Abdallah B M , Ali EM , Al-Ramadan SY, et al. (2024).** The Inhibitory Effect of Geraniol on CCL*4*-induced Hepatorenal Toxicity in Pregnant Mice through the PI3K/AKT Signaling Pathway. Saudi Journal of Medicine & Medical Sciences, *12*(1), 17-26.
- **Aziz WM , Hamed MA , Abd-Alla HI , Ahmed SA .(2022).** Pulicaria crispa mitigates nephrotoxicity induced by carbon tetrachloride in rats via regulation oxidative, inflammatory, tubular and glomerular indices. Biomarkers, *27*(1), 35-43.
- **Baig M , Khan MKA. (2023).** Renal toxicity induced by carbon tetrachloride in experimental model: Renal toxicity induced by ccl4 in experimental model. Pakistan BioMedical Journal, 30-35.
- **Bancroft JD , Layton C (2013)**. Theory and Practice of Histological Techniques. 7th Edition, Butterworth-Heinemann.
- **Barakat H , Almundarij T. (2020)**. Phenolic compounds and hepatoprotective potential of Anastatica hierochuntica ethanolic and aqueous extracts against CCl4-induced hepatotoxicity in rats. Journal of Traditional Chinese Medicine, *40*(6), 947.
- **Ben Mansour F , Ayadi H , van Pelt J , Elfeki A , Bellassoued K. (2024).** Antioxidant and Protective Effect of Ocimum basilicum Seeds Extract on Renal Toxicity Induced by Carbon Tetrachloride in Rats. Journal of Medicinal Food, 27(1), 60-71.
- **Bikbov B , Purcell C A , Levey A S , Smith M , Abdoli A , Abebe M , et al. (2020)**. Global, regional, and national burden of chronic kidney disease, 1990–2017: a systematic analysis for the Global Burden of Disease Study 2017. The lancet, 395(10225), 709-733.
- **Chen G , Zhang L , Wang X , Chen X. (2024)**. Autophagy, ferroptosis-related targets and renal function progression in patients with chronic kidney disease: bioinformatics analysis and experimental verification. Chinese Journal of Tissue Engineering Research, *28*(32), 5122.
- **Dai R , Zhang L , Jin H , Wang D , Cheng M , Sang T, et al. (2022).** Autophagy in renal fibrosis: Protection or promotion? , Frontiers in Pharmacology,*13*, 963920.
- **El-Refai HA , Saleh AM , Mohamed SI , Aboul Naser AF , Zaki RA , Gomaa SK , et al. (2024).** Biosynthesis of Zinc Oxide Nanoparticles Using Bacillus paramycoides for In Vitro Biological Activities and In Vivo Assessment Against Hepatorenal Injury Induced by CCl4 in Rats. Applied Biochemistry Biotechnology,1-21.
- **Feng X, Du W, Ding M, Zhao W, Xirefu X, Ma M , et al. (2022).** Myosin 1D and the branched actin network control the condensation of

p62 bodies. Cell Research, *32*(7), 659-669.

- **Gui Z, Suo C, Wang Z, Zheng M, Fei S, Chen H, et al. (2021).** Impaired ATG16L-dependent autophagy promotes renal interstitial fibrosis in chronic renal graft dysfunction through inducing EndMT by NF-κB signal pathway. Frontiers in Immunology, *12*, 650424.
- **Isogai S, Morimoto D, Arita K , Unzai S, Tenno T, Hasegawa J, et al. (2011)**. Crystal structure of the ubiquitin-associated (UBA) domain of p62 and its interaction with ubiquitin. Journal of Biological Chemistry, 286(36), 31864-31874.
- **Kageyama S, Gudmundsson SR , Sou Y-S, Ichimura Y, Tamura N , Kazuno S , et al. (2021)**. p62/SQSTM1-droplet serves as a platform for autophagosome formation and anti-oxidative stress response. Nature communications, *12*(1), 16.
- **Keith, DS, Nichols GA , Gullion CM , Brown JB , Smith D. (2004).** Longitudinal follow-up and outcomes among a population with chronic kidney disease in a large managed care organization. Archives of internal medicine, *164*(6), 659-663.
- **Kumar AV, Mills J , Lapierre LR. (2022)**. Selective autophagy receptor p62/SQSTM1, a pivotal player in stress and aging. Frontiers in Cell Developmental Biology, *10*, 793328.
- **Lamark T, Johansen T. (2021).** Mechanisms of selective autophagy. Annual review of cell
- developmental biology, *37*, 143-169.
- **Lamia SS, Emran T, Rikta JK, Chowdhury NI , Sarker M , Jain P , et al. (2021).** Coenzyme Q10 and silymarin reduce CCl4-induced oxidative stress and liver and kidney injury in ovariectomized rats—implications for protective therapy in chronic liver and kidney diseases. Pathophysiology, *28*(1), 50-63.
- **Li M , Luan F , Zhao Y , Hao H , Zhou Y, Han W, et al. (2016).** Epithelial-mesenchymal transition: An emerging target in tissue fibrosis. Experimental biology and medicine *241*(1), 1-13.
- **Li W , He P , Huang Y , Li F, Lu J , Li M , et al. (2021).** Selective autophagy of intracellular organelles: recent research advances. Theranostics *11*(1), 222.
- **Liang S , Wu Y-S , Li D-Y , Tang J-X , Liu H-F . (2022)**. Autophagy and renal fibrosis. Aging Disease ,*13*(3), 712.
- **Lin T-A , Wu VC-C , Wang C-Y. (2019)**. Autophagy in chronic kidney diseases.Cells, *8*(1), 61.
- **Lin T-Y , Hsu, Y-H. (2020)**. IL-20 in acute kidney injury: role in pathogenesis and potential as a therapeutic target. International journal of molecular sciences, *21*(3), 1009.
- **Ma J-Q , Zhang Y-J , Tian Z-K , Liu C-M .(2021).** Bixin attenuates carbon tetrachloride induced oxidative stress, inflammation and fibrosis in kidney by regulating the Nrf2/TLR4/MyD88 and PPAR-γ/TGF-β1/Smad3 pathway., International Immunopharmacology, *90*, 107117.
- **Matsumoto G , Wada K , Okuno M , Kurosawa M , Nukina N. (2011)**. Serine 403 phosphorylation of p62/SQSTM1 regulates selective autophagic clearance of ubiquitinated proteins. Molecular cell, *44*(2), 279-289.
- **Mizushima N , Levine B , Cuervo A M , Klionsky D. (2008).** Autophagy fights disease through cellular self-digestion. nature ,*451*(7182), 1069-1075.
- **Mizushima N , Levine B. (2020).** Autophagy in human diseases. New England journal of medicine, *383*(16), 1564-1576.
- **Mizushima N. (2018)**. A brief history of autophagy from cell biology to

physiology and disease. Nature cell biology *20*(5), 521-527.

- **Morsy BM, Hamed MA , Abd-Alla HI , Aziz WM , Kamel SN. (2021).** Downregulation of fibrosis and inflammatory signalling pathways in rats liver via Pulicaria crispa aerial parts ethanol extract. Biomarkers, *26*(8), 665-673.
- **Pohl C , Dikic I. (2019).** Cellular quality control by the ubiquitin-proteasome system and autophagy. Science *366*(6467), 818-822.
- **Que R , Cao M , Dai Y , Zhou Y , Chen Y , Lin L. (2022).** Decursin ameliorates carbon-tetrachloride-induced liver fibrosis by facilitating ferroptosis of hepatic stellate cells. Biochemistry Cell Biology Science, *100*(5), 378-386.
- **Ruiz-Ortega M , Rayego-Mateos S , Lamas S , Ortiz A , Rodrigues-Diez R . (2020).** Targeting the progression of chronic kidney disease. Nature Reviews Nephrology, *16*(5), 269-288.
- **Sheng L , Zhuang S. (2020)**. New insights into the role and mechanism of partial epithelial-mesenchymal transition in kidney fibrosis. Frontiers in physiology, *11*, 569322.
- **Shi Q , Xia Y , Wu M , Pan Y , Wu S , Lin J, et al. (2024).** Mi-BMSCs alleviate inflammation and fibrosis in CCl4-and TAA-induced liver cirrhosis by inhibiting TGF-β/Smad signaling. Materials Today Bio ,100958.
- **Shu S , Wang H , Zhu J , Liu Z , Yang D , Wu W, et al. (2021).** Reciprocal regulation between ER stress and autophagy in renal tubular fibrosis and apoptosis. Cell death disease *12*(11), 1016.
- **Singh S , Nirala SK , Bhadauria M. (2024).** Comparative role of acetaminophen, carbon tetrachloride and thioacetamide in development of fibrosis in rats. Toxicology Research, *13*(1), tfad114.
- **Sun D , Wu R , Zheng J , Li P , Yu L. (2018).** Polyubiquitin chain-induced p62 phase separation drives autophagic cargo segregation. Cell research 28(4), 405-415.
- **Susilo R J K , Winarni D , Hayaza S , Doong R-A , Wahyuningsih S P A , Darmanto W. (2022).** Effect of crude Ganoderma applanatum polysaccharides as a renoprotective agent against carbon tetrachloride-induced early kidney fibrosis in mice. Veterinary World, *15*(4), 1022.
- **Tan J , Wang M , Song S , Miao Y , Zhang Q. (2018)**. Autophagy activation promotes removal of damaged mitochondria and protects against renal tubular injury induced by albumin overload.Histology and Histopathology, 33(7),736-746.
- **Tang C , Livingston M J , Liu Z , Dong Z. (2020).** Autophagy in kidney homeostasis and disease. Nature Reviews Nephrology, *16*(9), 489-508.
- **Unsal V , Cicek M , Sabancilar I . (2021).** Toxicity of carbon tetrachloride, free radicals and role of antioxidants. Reviews on environmental health, *36*(2), 279-295.
- **Yeh Y-H , Hsieh Y-L , Lee Y-T . (2013).** Effects of yam peel extract against carbon tetrachloride-induced hepatotoxicity in rats. Journal of Agricultural Food Chemistry, *61*(30), 7387-7396.
- **Zhao Y , Zhao M , Wang Z , Zhao C , Zhang Y, Wang M. (2024).** Danggui Shaoyao San: Chemical characterization and inhibition of oxidative stress and inflammation to treat CCl4-induced hepatic fibrosis. Journal of Ethnopharmacology, *318*, 116870.
- **Zheng C, Zhou Y , Huang Y , Chen B , Wu M , Xie Y, et al. (2019).** Effect of ATM on inflammatory response and autophagy in renal tubular epithelial cells in LPS‐induced septic AKI. Experimental therapeutic medicine , *18*(6), 4707-4717.